

Intramolecular N–H...O Hydrogen Bonding Assisted by Resonance. Part 2.¹ Intercorrelation between Structural and Spectroscopic Parameters for Five 1,3-Diketone Arylhydrazones Derived from Dibenzoylmethane

Valerio Bertolasi,^a Valeria Ferretti,^a Paola Gilli,^a Gastone Gilli,^{*,a} Y. M. Issa^b and O. E. Sherif^b

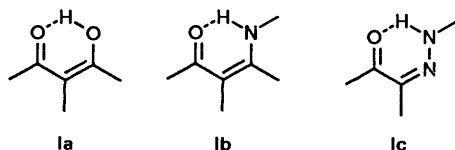
^a Centro di Strutturistica Diffrattometrica and Dipartimento di Chimica, Università di Ferrara, 44100 Ferrara, Italy

^b Chemistry Department, Faculty of Science, Cairo University, Cairo, Egypt

The crystal structures of five propane-1,2,3-trione arylhydrazones are reported. All molecules are chelated to form a six-membered π -conjugated ring *via* strong intramolecular N–H...O hydrogen bonding. The N...O hydrogen bond distances are correlated with the resonance entity within the ring and with spectroscopic data such as $\nu(\text{NH})$ IR frequencies $\delta(\text{NH})$ ¹H NMR chemical shifts and λ_{max} UV absorption bands of charge transfer from hydrazone to carbonyl group. The structural and spectroscopic variations of the hydrogen bond parameters are modulated by the electronic properties of substituents on the aryl group in the sense that electron donating groups produce the strongest hydrogen bonds. The intercorrelation between N...O hydrogen bond strength and π delocalization in all the structures of this class retrieved from the Cambridge Structural Database shows that the interplay between π resonance and hydrogen bond magnitude, which we have called Resonance Assisted Hydrogen Bonding (RAHB), is a general phenomenon in the whole class of 1,3-diketone arylhydrazones.

Extensive experimental and theoretical efforts have been devoted to understanding the reasons for the formation of the very strong intramolecular O–H...O hydrogen bond in β -diketo enol systems (**1a**).² Recently, a model called RAHB (Resonance Assisted Hydrogen Bond) was suggested, which is essentially a synergistic mutual reinforcement of hydrogen bonding and π delocalization within the heterodienic system.³ This model has been successfully employed to interpret both the intra- and inter-molecular hydrogen bonds in all the compounds containing the β -diketo enol fragment.

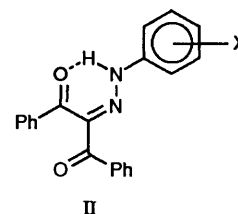
Since the introduction of the concept of RAHB, we have foreseen the existence of strong intramolecular hydrogen bonds formed by other fragments, which display similar resonance along the π -conjugated atomic chain, such as enamines (**1b**), keto-hydrazones (**1c**), *etc.* In order to verify this prediction we



have undertaken crystal and spectroscopic studies on a series of 1,3-diketone arylhydrazones, which are known to present very strong intramolecular hydrogen bonds having N...O distances as short as 2.55 Å, low $\nu(\text{NH})$ IR frequencies around 3000 cm^{-1} and high $\delta(\text{NH})$ ¹H NMR chemical shifts up to 15.9.^{1,4}

Previous structural and spectroscopic data¹ collected for a series of 1,3-diketone arylhydrazones derived from benzoylacetone or acetylacetone have already indicated that the magnitude of the strong hydrogen bond formed is essentially determined by the degree of resonance within the heterodienic system modulated by the inductive effects of the aryl substituents. In this paper the crystal structures and spectroscopic data for the other five compounds belonging to the same class but derived from dibenzoylmethane (**II**) are reported together with a survey of the crystal structures of 1,3-diketone

arylhydrazone derivatives, retrieved from the Cambridge Structural Database (CSD),⁵ with the purpose of showing that the RAHB model is able to interpret the hydrogen bond magnitude in this class of compound.



- | | |
|----------------------------------|----------------------------------|
| 1 X = <i>m</i> -NO ₂ | 4 X = H |
| 2 X = <i>p</i> -CH ₃ | 5 X = <i>p</i> -OCH ₃ |
| 3 X = <i>o</i> -OCH ₃ | |

Experimental

The detailed synthesis of the five 1,3-diketone arylhydrazones, carried out by coupling diazonium salts with dibenzoylmethane, have been reported elsewhere.⁶ The compounds were recrystallized from mixtures of CHCl₃–CH₃OH–C₂H₅OH.

Crystal data, data collection and refinement details are given in Table 1. All X-ray diffraction data were collected at room temp. on an Enraf–Nonius CAD4 diffractometer using graphite monochromated Mo–K α radiation ($\lambda = 0.71069$ Å) with $\omega/2\theta$ scan technique. Lattice constants were determined by least squares fitting of the setting angles of 25 reflections in the range $10 \leq \theta \leq 15^\circ$. Intensities of three standard reflections were measured every 2 h and did not show significant variations for any of the five compounds investigated. All intensities were collected in the range $2 \leq \theta \leq 28^\circ$ and corrected for Lorentz and polarization. Scattering factors were taken from ref. 7. The structures were solved by direct methods with the SIR88^{8a} system of programs and all other calculations were accomplished by the MolEN^{8b} system of programs and PARST.^{8c} All structures were refined by full matrix least squares, with all non-H atoms anisotropic and all H-atoms isotropic. H-atom

Table 1 Crystal data

Compound	1	2	3	4	5
Formula	C ₂₁ H ₁₅ N ₃ O ₄	C ₂₂ H ₁₈ N ₂ O ₂	C ₂₂ H ₁₈ N ₂ O ₃	C ₂₁ H ₁₆ N ₂ O ₂	C ₂₂ H ₁₈ N ₂ O ₃
<i>M</i>	373.4	342.4	358.4	328.4	358.4
Space group	<i>P</i> 2 ₁ / <i>n</i>	<i>P</i> 2 ₁ / <i>n</i>	<i>P</i> 2 ₁ / <i>n</i>	<i>P</i> 2 ₁ / <i>n</i>	<i>P</i> 2 ₁
Crystal system	monoclinic	monoclinic	monoclinic	monoclinic	monoclinic
<i>a</i> /Å	10.581(3)	12.273(2)	11.102(3)	9.799(4)	5.918(2)
<i>b</i> /Å	10.548(1)	10.301(3)	11.174(2)	10.237(2)	16.451(2)
<i>c</i> /Å	16.459(2)	14.259(2)	15.697(5)	17.307(2)	9.406(1)
β /°	102.40(2)	96.23(1)	108.51(2)	102.26(2)	97.56(2)
<i>V</i> /Å ³	1794.1(6)	1792.0(6)	1846.5(9)	1696.5(8)	907.8(3)
<i>Z</i>	4	4	4	4	2
<i>D</i> _c /g cm ⁻³	1.38	1.27	1.29	1.28	1.31
<i>F</i> (000)	776	720	752	688	376
μ (Mo-K α)/cm ⁻¹	0.9	0.8	0.8	0.8	0.8
Crystal size/mm ³	0.17 × 0.22 × 0.43	0.26 × 0.28 × 0.52	0.26 × 0.31 × 0.38	0.14 × 0.26 × 0.43	0.13 × 0.31 × 0.45
Independent reflections	4307	4313	4444	4088	2255
Observed reflections (<i>N</i> _o)	2034 [<i>I</i> > 3 σ (<i>I</i>)]	2339 [<i>I</i> > 2 σ (<i>I</i>)]	2232 [<i>I</i> > 3 σ (<i>I</i>)]	1668 [<i>I</i> > 3 σ (<i>I</i>)]	1814 [<i>I</i> > 2 σ (<i>I</i>)]
<i>R</i> ^a	0.044	0.042	0.042	0.038	0.034
<i>R</i> _w ^b	0.053	0.050	0.048	0.040	0.041
<i>p</i> ^c	0.04	0.03	0.04	0.03	0.04
<i>N</i> _o / <i>N</i> _v	6.5	7.6	7.1	5.8	5.8
Max. shift/error	0.02	0.03	0.01	0.01	0.01
No. of variables (<i>N</i> _v) (last cycle)	313	307	316	290	315
GOF ^d	1.6	1.8	1.5	1.4	1.4
Largest ΔF peak/e Å ⁻³	0.16	0.16	0.13	0.11	0.12

^a $R = \sum |\Delta F| / \sum |F_o|$. ^b $R_w = [\sum (\Delta F)^2 / \sum w(F_o)^2]^{\frac{1}{2}}$. ^c $w = 4F_o^2 / [\sigma^2 F_o^2 + (pF_o)^2]$. ^d $GOF = [\sum (\Delta F)^2 / (N_o - N_v)]^{\frac{1}{2}}$.

Table 2 Selected bond distances (Å), bond angles (°) and torsion angles (°) with esds in parentheses

	1	2	3	4	5
N(1)–N(2)	1.322(3)	1.311(2)	1.307(2)	1.316(2)	1.293(2)
N(2)–C(7)	1.313(2)	1.324(2)	1.318(2)	1.310(2)	1.336(2)
C(7)–C(8)	1.482(3)	1.475(2)	1.472(3)	1.470(3)	1.464(2)
C(8)–O(1)	1.225(3)	1.232(2)	1.237(2)	1.229(3)	1.234(2)
N(1)–C(5)	1.401(2)	1.400(2)	1.403(2)	1.391(2)	1.410(2)
C(7)–C(9)	1.497(3)	1.485(3)	1.485(3)	1.488(3)	1.478(2)
C(9)–O(2)	1.222(3)	1.222(2)	1.219(2)	1.222(2)	1.222(2)
C(5)–N(1)–N(2)	119.8(2)	121.8(1)	119.6(2)	119.3(2)	121.0(2)
N(1)–N(2)–C(7)	120.3(2)	119.5(1)	121.4(2)	121.1(2)	120.4(2)
N(2)–C(7)–C(8)	124.7(2)	123.8(2)	124.0(2)	125.0(2)	123.4(2)
C(7)–C(8)–O(1)	119.9(2)	120.3(2)	119.1(2)	119.2(2)	120.4(2)
N(2)–C(7)–C(9)	114.9(2)	115.5(1)	112.7(2)	113.1(2)	114.0(2)
C(8)–C(7)–C(9)	119.6(2)	120.1(2)	122.6(2)	121.5(2)	122.1(2)
O(1)–C(8)–C(7)–N(2)	–15.1(3)	–15.5(3)	3.6(3)	14.7(3)	8.0(3)
C(8)–C(7)–N(2)–N(1)	4.8(3)	5.6(3)	0.4(3)	–7.3(2)	0.4(3)
C(7)–N(2)–N(1)–C(5)	179.6(2)	–176.2(2)	–177.6(2)	178.5(2)	–179.8(2)
C(8)–C(7)–C(9)–O(2)	–32.8(3)	–30.6(2)	24.8(3)	40.3(3)	18.3(3)
N(2)–N(1)–C(5)–C(4) w1	–161.9(2)	–166.3(2)	178.0(2)	154.4(2)	–178.8(2)
N(2)–N(1)–C(5)–C(6) w2	18.8(3)	14.0(2)	1.6(3)	–27.1(3)	3.1(3)
τ	18.4	13.8	1.8	26.4	2.2

^a $\tau = |w1 + w2 \pm 180|/2$.

positions were determined from the ΔF synthesis carried out after the first cycles of isotropic refinement.

IR spectra were recorded on a Nicolet 510P FTIR spectrometer from KBr pellets and ¹H NMR spectra in a solution of CDCl₃ on a Gemini 300 Varian instrument.

Results and Discussion

A selection of bond distances, bond angles and torsion angles are reported in Table 2. Hydrogen bond parameters are given in Table 3. ORTEP⁹ views of the molecules, projected onto the hydrazone plane, are shown in Fig. 1.*

All molecules display similar configurations and conformations which can be represented as *EZE*, where *E* and *Z* are used to describe, in order, the alignments of the free C(9)=O(2)

and of the hydrogen bonded C(8)=O(1) double bonds and of the C(1)–C(6) aryl group with respect to the C(7)=N(2) double bond.¹⁰

In this arrangement the partial charges generated by the π conjugation on the N(1) and O(1) atoms should be quenched by the formation of the hydrogen bond (IIIa), by analogy to what occurs in the β -diketo enol system (IIIb). Owing to the presence of two ketonic groups, however, the total charge redistribution is more complex and can be interpreted in terms of the

* Tables of bond distances and angles, thermal parameters and atom co-ordinates have been deposited at the Cambridge Crystallographic Data Centre. For details, see 'Instructions for Authors (1993)', *J. Chem. Soc., Perkin Trans. 2*, 1993, issue 1.

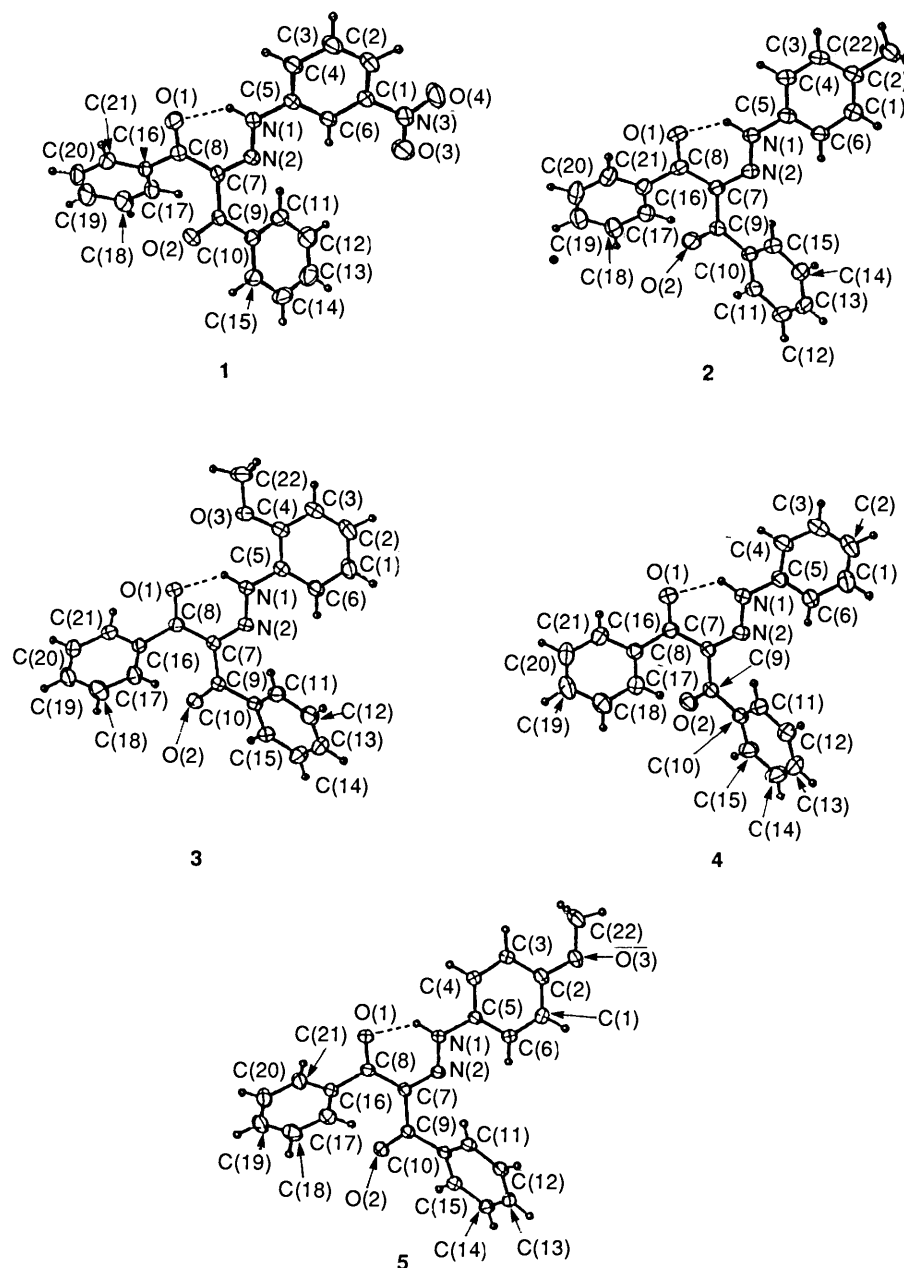
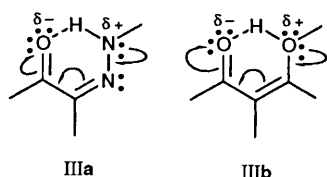


Fig. 1 ORTEP⁹ views of the molecules 1–5 showing the thermal ellipsoids at 30% probability

contributions of the four IVa–IVd forms, where the contribution of the polar form IVb to the ground state of the molecule is the most important ($\approx 35\%$ on average, calculated using the bond order concept),¹¹ while the contribution of the form IVc is smaller ($\approx 15\%$) and that of the form IVd only marginal ($\approx 5\%$).



Because the two adjacent C(7)=N(2) and N(2)–N(1) bonds are involved in all the three polar forms IVb–d, a more proper description of global delocalization within the N(1)–N(2)=C(7)–C(8)=O(1) conjugated chain is obtained by an empirical parameter Λ derived from the changes of the C(7)=N(2) and N(1)–N(2) experimental bond distances with respect to the

standard ones [$d(\text{C}=\text{N}) = 1.279$ and $d(\text{N}–\text{N}) = 1.401$ Å in planar systems].¹² The parameter Λ is defined as $\Lambda = (1 + q/Q)/2$, where q is the difference $d[\text{N}(1)–\text{N}(2)] - d[\text{N}(2)=\text{C}(7)]$ between the actual distances and Q is the same difference between the standard values, *i.e.* 0.122 Å. Λ is calculated to be 0.484 for a complete π delocalization, while for a system with pure double and single bonds, it assumes the values of 1 or 0.029 for the C=N–N and C–N=N situations, respectively. Table 4 reports the N(1)···O(1) contact distances, the resonance parameters Λ as well as the ¹H NMR chemical shifts, $\delta(\text{H})$, the IR stretching frequencies, $\nu(\text{NH})$, λ_{max} of the UV absorption band for the charge transfer (CT) from the hydrazone to the carbonyl group, and the Hammett constants, $\sigma(\text{X})$,¹³ for the phenyl substituent X in II. To stress the unusual features of these hydrogen bonds, it can be observed that the N(1)···O(1) lengths [2.565(2)–2.612(3) Å] are much shorter than the average value of 2.755 Å calculated from a statistical analysis over 152 intramolecular N–H···O hydrogen bonds.¹⁴ On the other hand, the experimental values of $\nu(\text{NH})$ and $\delta(\text{NH})$ (in the ranges of 2999–3166 cm⁻¹ and 13.28–13.97, respectively) are rather

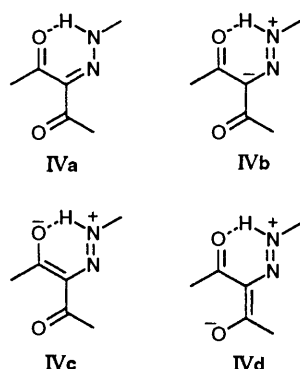
Table 3 Hydrogen bond parameters (Å and °) with esds in parentheses

	N(1)–H(1N)	N(1)···O(1)	H(1N)···O(1)	N(1)–H(1N)···O(1)
1	0.89(2)	2.612(3)	1.94(2)	131(2)
2	0.97(1)	2.575(2)	1.77(2)	138(1)
3	0.89(2)	2.567(2)	1.88(2)	132(2)
4	0.91(2)	2.609(3)	1.95(2)	128(2)
5	0.91(2)	2.565(2)	1.84(2)	135(2)

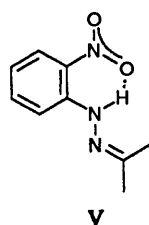
Table 4 Summary of crystal and spectroscopic data for compounds 1–5 ordered for increasing N···O distances

Compound	$d(\text{N}\cdots\text{O})/\text{Å}$	X	Λ^a	σ^b	$\nu(\text{N-H})^c/\text{cm}^{-1}$	$\delta(\text{N-H})^d$	$\lambda_{\text{max}}^e/\text{nm}$
5	2.565(2)	<i>p</i> -OMe	0.32	–0.28	3058	13.97	418
3	2.567(2)	<i>o</i> -OMe	0.46	–0.28	3059	13.74	418
2	2.575(2)	<i>p</i> -Me	0.45	–0.17	2999	13.75	402
4	2.609(3)	H	0.52	0	3160	13.60	382
1	2.612(3)	<i>m</i> -NO ₂	0.54	0.71	3166	13.8	385
r^f			0.82	0.82	0.88	–0.86	–0.97

^a As defined in the text. ^b Hammett constants from ref. 13. ^c Measured as KBr pellets. ^d Measured in CDCl₃. ^e Measured in ethanol. ^f Correlation coefficients for the linear regressions of the various parameters *vs.* $d(\text{N}\cdots\text{O})$.

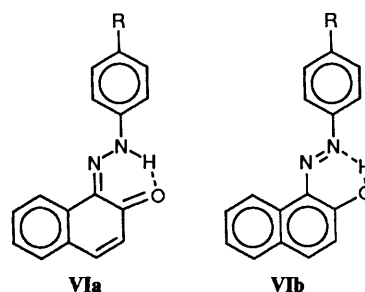


different, for example, from the values of 3285–3385 cm^{–1} and 10.7–11.5 found in some arylhydrazones which form reasonably strong intramolecular hydrogen bonds [$2.61 \leq d(\text{N}\cdots\text{O}) \leq 2.64 \text{ Å}$] with an *o*-nitro group on the phenyl ring (V).^{15,16}



The last line of Table 4 reports the values of the correlation coefficients, r , for the dependence of the different parameters on the N(1)···O(1) hydrogen bond distance. They are in agreement with those already calculated in a previous paper¹ for similar compounds. The correlation of the Hammett constant $\sigma(\text{X})$ with the $d(\text{N}\cdots\text{O})$ distance ($r = 0.82$) (and, in turn, with all other parameters) suggests that the electronic properties of the X-substituent can modulate the structural and spectroscopic parameters related to the hydrogen bond. These electronic effects can be considered essentially inductive in nature owing to the lack of shortening of the C(5)–N(1) bond distances and of quinoid character of the C(1)–C(6) phenyl ring, in spite of the planarity of the arylhydrazone moiety [the dihedral angles τ between the hydrazone and phenyl groups are in the range 1.8–26.4° (Table 2)]. The fact that electron withdrawing substituents tend to lengthen the N(1)···O(1)

hydrogen bond distance, to decrease $\delta(\text{NH})$ and λ_{max} , and to increase $\nu(\text{NH})$ may be explained because they increase the positive charge on N(1) by a mechanism which is coming into conflict with the synergistic RAHB process (IIIa). Opposite effects are produced by electron donating groups. A similar modulation of the hydrogen bond properties by an X substituent occurs in 1,2-naphthoquinone arylhydrazones (VIa) which are in tautomeric equilibrium with 1-aryloxy-2-naphthols (VIb). In general, the 'hydrazone' form VIa is preferred with respect to the 'azo' form VIb;¹⁷ however, in the case of the dimethylamino derivative ($\text{R} = \text{NMe}_2$), the form VIb becomes more stable probably because the strongly electron donating group, [$\sigma_p(\text{Hammett}) = -0.63$] makes the hydrogen bond so strong that the proton can be intramolecularly transferred from nitrogen to oxygen shifting the equilibrium towards the 'azo' tautomer, which is accordingly that observed in the solid state.¹⁸



The influence of the electronic properties of X on the conjugated heterodienic keto-hydrazone moiety has been well established by previous studies⁶ which have proved a strict correlation between $\sigma(\text{X})$ and UV λ_{max} for CT between the hydrazone and the keto group in a large series of 1,3-diketone arylhydrazones. The negative sign of the λ_{max} *vs.* $\sigma(\text{X})$ correlation indicates that a lower energy is required for this CT transition, in agreement with the observed shortening of the hydrogen bonding and increased π delocalization.

In order to show that the interplay between π resonance and hydrogen bond strengthening (what we have called RAHB) is a general phenomenon in the whole class of 1,3-diketone arylhydrazones, a systematic search of CSD structural data for these compounds was carried out. The search was limited to the situation where the heteroconjugated keto-hydrazone moiety

Table 5 Structural data retrieved from Cambridge Structural Database (CSD)⁵ and available IR spectroscopic data for 1,3-diketone arylhydrazones divided into groups according to VII

REFCODE ^a	$d[\text{N}(1)\cdots\text{O}(1)]/\text{\AA}$	Λ	$\nu(\text{NH})/\text{cm}^{-1}$	$d[\text{N}(3)\cdots\text{O}(2)]/\text{\AA}$	Ref.
VIIa					
h1	2.581(2)	0.41	3057	—	1
h2A	2.551(5)	0.41	3002	—	1
h2B	2.591(5)	0.44	3108	—	1
<h2>	<2.571> ^b	<0.42>	—	—	1
h3	2.559(3)	0.39	3058	—	1
h4	2.561(3)	0.40	3067	—	1
h5	2.598(3)	0.56	3117	—	1
h6	2.600(2)	0.48	3117	—	1
NPHDZC	2.57(1)	0.48	3130	—	16
MENDND10	2.70(1)	0.76	3200	—	16
ECPHOP	2.68(2)	0.64	3228	—	19
ECPHOP	2.58(2)	0.47	—	—	19
BERNUH	2.559(5)	0.46	3140	—	20
BERPAP	2.64(1)	0.64	3164	—	20
VIIb					
NCPAAA01	2.591(2)	0.58	—	2.666(2)	21
QQQEK10	2.60(1)	0.57	—	2.64(1)	22
CEWGOA	2.564(8)	0.46	—	2.650(8)	23
CEWGUG	2.576(3)	0.50	—	2.684(3)	23
QQQAZG21	2.605(8)	0.54	—	2.664(8)	24
QQQAZG02	2.596(5)	0.51	—	2.661(5)	25
QQQAZG03	2.596(3)	0.56	—	2.656(3)	26
DANDIF	2.610(3)	0.65	—	2.659(4)	27
FOVNOT	2.572(3)	0.51	—	2.642(3)	28
DIFFON	2.590(4)	0.52	—	2.662(4)	29
QQQELA03	2.567(3)	0.54	—	2.661(2)	30
DIPVUT	2.557(6)	0.46	—	2.692(6)	31
DUXXID	2.593(3)	0.56	—	2.654(3)	32
FUCTUS	2.597(3)	0.57	—	2.657(3)	33
FUCTOM	2.562(3)	0.50	—	2.666(3)	34

^a Codes according to CSD⁵ except those indicated as h1–h6 which refer to the structures reported in the previous paper.¹ ^b < > Average values.

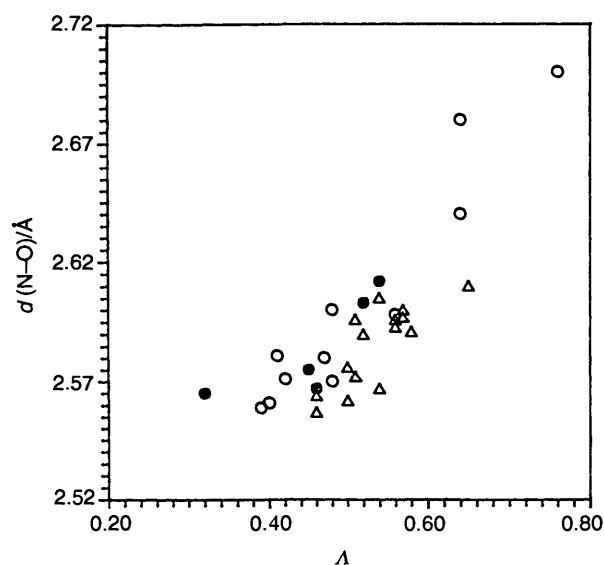


Fig. 2 Scatter plot of the bond distance $d(\text{N}\cdots\text{O})$ vs. resonance parameter Λ : ●, the present compounds; ○, compounds VIIa; △, compounds VIIb (from Table 5). Linear regression $r = 0.82$.

was not part of a ring, thereby avoiding intramolecular constraints. The molecules found were classified as shown in VIIa and VIIb. Compounds of group VIIa include the structures described by us in the present and in a previous paper.¹ In compounds VIIb, the 1,3-diketo fragment is substituted by a 3-oxopropanamide moiety, and a further intramolecular hydrogen bond between the amidic N(3)–H and O(2) is observed. The relevant parameters are summarized in Table 5. Fig. 2 reports the scatter plot Λ vs. $d(\text{N}\cdots\text{O})$. The intercorrelation

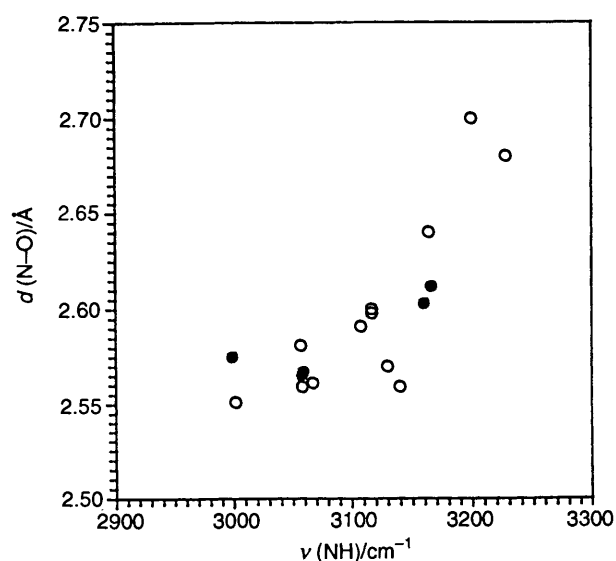
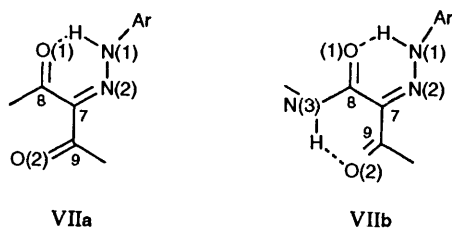


Fig. 3 Scatter plot of the bond distance $d(\text{N}\cdots\text{O})$ vs. IR stretching frequency $\nu(\text{NH})$: ●, the present compounds; ○, compounds VIIa (from Table 5). Linear regression $r = 0.80$.

between these two quantities clearly shows a dependence of the N(1)⋯O(1) hydrogen bond strength on the π delocalization in agreement with the RAHB model. Strictly similar indications can be obtained from the correlation between N(1)⋯O(1) and the available values of $\nu(\text{NH})$ (Fig. 3), confirming that the IR stretching frequencies are, in general, quite good indicators of the hydrogen bond magnitude.

The importance of conjugation in determining the intramolecular hydrogen bond strength is, on the other hand, further



illustrated by comparing $N(1) \cdots O(1)$ with $N(3) \cdots O(2)$ distances in compounds VIIb. The $N(1)$ and $O(1)$ atoms belong to a heteroconjugated system and their distances average to 2.585(17) Å; they are systematically shorter than the $N(3) \cdots O(2)$ distances [average value of 2.661(14) Å]. These larger values are not justifiable in terms of intramolecular constraints but only in terms of a lack of conjugation within the intramolecularly six-membered $N(3)-C(8)-C(7)-C(9)=O(2)$ hydrogen bonded system.

Acknowledgements

We thank *Ministero Università e Ricerca Scientifica e Tecnologica*, Italy, for financial support.

References

- Part I. V. Bertolasi, L. Nanni, P. Gilli, V. Ferretti, G. Gilli, Y. M. Issa and O. E. Sherif, *New J. Chem.*, 1994, in press.
- (a) J. Emsley, *Struct. Bonding*, 1984, **57**, 147; (b) M. C. Etter and G. M. Vojta, *J. Mol. Graphics*, 1989, **7**, 3; (c) T. S. Kopleva and D. N. Shigorin, *Russ. J. Phys. Chem.*, 1974, **48**, 312; (d) M. J. Frisch, A. C. Schneider, H. F. Schaefer III and J. S. Binkley, *J. Chem. Phys.*, 1985, **82**, 4194; (e) A. J. Vila, C. M. Lagier and A. C. Olivieri, *J. Chem. Soc., Perkin Trans. 2*, 1990, 1615.
- (a) G. Gilli, F. Bellucci, V. Ferretti and V. Bertolasi, *J. Am. Chem. Soc.*, 1989, **111**, 1023; (b) V. Bertolasi, P. Gilli, V. Ferretti and G. Gilli, *J. Am. Chem. Soc.*, 1991, **113**, 4917; (c) G. Gilli and V. Bertolasi in *The Chemistry of Enols*, ed. Z. Rappoport, Wiley, New York, 1990, p. 713; (d) G. Gilli, V. Bertolasi, V. Ferretti and P. Gilli, *Acta Crystallogr., Sect. B*, 1993, **49**, 564.
- (a) A. Mitchell and D. C. Nonhebel, *Tetrahedron*, 1979, **35**, 2013; (b) F. Kaberia, B. Vickery, G. R. Willey and M. G. B. Drew, *J. Chem. Soc., Perkin Trans. 2*, 1980, 1622; (c) M. G. B. Drew and G. R. Willey, *Educ. Chem.*, 1985, **22**, 106.
- F. H. Allen, S. Bellard, M. D. Brice, B. A. Cartwright, A. Doubleday, H. Higgs, T. Hummelink, B. G. Hummelink-Peters, O. Kennard, W. D. S. Motherwell, J. R. Rogers and D. G. Watson, *Acta Crystallogr., Sect. B*, 1979, **35**, 2331.
- A. K. El-Ansary, Y. M. Issa and H. A. Mohamed, *Kolor. Ert.*, 1987, **5**, 141.
- International Tables for X-Ray Crystallography*, Kynoch Press, Birmingham, 1974, vol. 4, p. 71.
- (a) M. C. Burla, M. Camalli, G. Cascarano, C. Giacovazzo, G. Polidori, R. Spagna and D. Viterbo, SIR88, A Direct Methods Program for the Automatic Solution of Crystal Structures, *J. Appl. Crystallogr.*, 1989, **22**, 389; (b) MolEN, An Interactive Structure Solution Procedure, Enraf-Nonius, Delft, The Netherlands, 1990; (c) M. Mardelli, *Comput. Chem.*, 1983, **7**, 95.
- C. J. Johnson, ORTEP II, A Fortran Thermal-Ellipsoids Plot Program for Crystal Structures Illustrations, Report ORNL-5138, Oak Ridge National Laboratory, Oak Ridge, Tennessee, 1976.
- A. Gomez-Sanchez, M. G. Garcia Martin, P. Borrachero and J. Bellanato, *J. Chem. Soc., Perkin Trans. 2*, 1987, 301.
- L. Pauling, *J. Am. Chem. Soc.*, 1947, **69**, 542.
- F. H. Allen, O. Kennard, D. G. Watson, L. Bremmer, G. Orpen and R. Taylor, *J. Chem. Soc., Perkin Trans. 2*, 1987, S1.
- J. Shorter in *Similarity Models in Organic Chemistry, Biochemistry and Related Fields*, eds. R. I. Zalewski, T. M. Krygowski and J. Shorter, Elsevier, Amsterdam, 1991, ch. 2.
- R. Taylor, O. Kennard and W. Versichel, *Acta Crystallogr., Sect. B*, 1984, **40**, 280.
- (a) G. R. Willey and M. G. B. Drew, *Acta Crystallogr., Sect. C*, 1985, **41**, 589; (b) M. G. B. Drew and G. R. Willey, *J. Chem. Soc., Perkin Trans. 2*, 1986, 215.
- B. Vickery, G. R. Willey and M. G. B. Drew, *J. Chem. Soc., Perkin Trans. 2*, 1981, 155.
- J. E. Kuder, *Tetrahedron*, 1972, **28**, 1973.
- A. C. Olivieri, R. B. Wilson, I. C. Paul and D. Y. Curtin, *J. Am. Chem. Soc.*, 1989, **111**, 5525.
- M. G. B. Drew, B. Vickery and G. R. Willey, *Acta Crystallogr., Sect. B*, 1981, **37**, 992.
- M. G. B. Drew, B. Vickery and G. R. Willey, *Acta Crystallogr., Sect. B*, 1982, **38**, 1530.
- A. Whitaker, *Z. Kristallogr.*, 1983, **163**, 139.
- A. Whitaker, *Z. Kristallogr.*, 1983, **163**, 19.
- E. F. Paulus, W. Rieper and D. Wagner, *Z. Kristallogr.*, 1983, **165**, 137.
- A. Whitaker, *Z. Kristallogr.*, 1984, **166**, 177.
- C. J. Brown and R. Yadav, *Acta Crystallogr., Sect. C*, 1984, **40**, 564.
- E. F. Paulus, *Z. Kristallogr.*, 1984, **167**, 65.
- A. Whitaker, *Z. Kristallogr.*, 1984, **167**, 225.
- A. Whitaker, *Z. Kristallogr.*, 1985, **171**, 17.
- A. Whitaker, *Z. Kristallogr.*, 1985, **170**, 213.
- A. Whitaker and N. Walker, *Z. Kristallogr.*, 1985, **171**, 7.
- S. Mehdi, Y. S. Sadanandam, M. M. Shetty and B. Rama Rao, *Acta Crystallogr., Sect. C*, 1986, **42**, 347.
- A. Whitaker, *Acta Crystallogr., Sect. C*, 1986, **42**, 1566.
- A. Whitaker and N. P. C. Walker, *Acta Crystallogr., Sect. C*, 1987, **43**, 2137.
- A. Whitaker, *Acta Crystallogr., Sect. C*, 1987, **43**, 2141.

Paper 3/03526C

Received 18th June 1993

Accepted 14th July 1993